

Pulsed Discharge in a Hollow Cathode with the Detection of Ions in a Time-of-Flight Mass Spectrometer: Analytical Capabilities in the Analysis of Solid Samples

A. A. Ganeev^a, M. A. Kuz'menkov^a, V. A. Lyubimtsev^b, S. V. Potapov^b,
A. I. Drobyshev^a, S. S. Potemin^b, and M. V. Voronov^b

^a St. Petersburg State University (Petrodvorets Branch), Universitetskii pr. 26, Petrodvorets, 198504 Russia

^b NPF Lyumeks, Moskovskii pr. 19, St. Petersburg, 190005 Russia

Received November 11, 2005; in final form, July 7, 2006

Abstract—The results of a study of a new analytical system that includes an ion source with a hollow-cathode pulsed gas discharge and a time-of-flight mass spectrometer are reported. It was found that such a system can be successfully used for the direct analysis of metal and dielectric solid samples. The results of the optimization of various ionizer parameters, such as the delay of an ejecting pulse with respect to a discharge pulse and the bias voltage of the anode–cathode pair, are given. It was proposed to use an additive of hydrogen as a reaction gas for a considerable decrease in the intensities of gas components in the mass spectrum, and the effectiveness of this approach was demonstrated. The possibility of the rapid and efficient direct analysis of solid samples with the use of a hollow-cathode pulsed glow discharge was demonstrated using an example of the analysis of high-purity copper samples and the glassy slag of molten lead.

DOI: 10.1134/S1061934807050097

Various versions of a glow discharge are used as spectrum excitation sources in atomic emission spectrometry [1–3] and as ion sources in mass spectrometry [4–13]. The glow discharge provides an opportunity to analyze solid and powder samples, as well as to perform layer-by-layer analysis [1, 2, 9].

The following two main types of glow-discharge ion sources, which are used for the analysis of solid samples, are well known: a flat-cathode glow discharge (Grimm discharge) [14] and a hollow-cathode glow discharge [5]. As compared with the Grimm discharge, the rate of sample sputtering is higher and the ionization of sputtered atoms is more efficient in the hollow-cathode discharge. A hollow-cathode pulsed discharge further enhances the rates of sputtering and ionization. Moreover, the pulsed discharge considerably suppresses gas components that interfere with the determination of a number of elements by time discrimination [11, 12].

Of well-known mass-spectrometric systems, a time-of-flight mass spectrometer is best suited for operation with pulsed ion sources because the greatest efficiency of the detection of sample ions takes place in this case [4–6]. The time-of-flight mass spectrometry with a pulsed discharge in a hollow-cathode cell (Grimm discharge) has been studied in a number of works [15, 16]. A version with double discharge pulses has been proposed and implemented [17]. The first pulse sputtered the sample, and the second pulse efficiently ionized it. As a result, the ion signal from sample elements considerably increased. In this case, although the discharge

current increased to several hundreds of milliamperes, the average current was very low: fractions of a milliampere (because of a low pulse frequency). The use of a hollow-cathode pulsed discharge in place of the Grimm pulsed discharge will significantly improve the analytical characteristics of a system with time-of-flight ion detection. In all of these works, the analytical parameters obtained did not allow pulsed-discharge time-of-flight mass spectrometry to compete successfully with other techniques for the direct analysis of solid samples, such as glow-discharge optical spectrometry [1, 18, 19], inductively coupled laser ablation [20, 21], and radiofrequency-discharge sector mass spectrometry [22–24].

This work was devoted to the study of the analytical characteristics of a new version of time-of-flight mass spectrometry with sample ionization in a hollow-cathode pulsed discharge for the analysis of conducting and nonconducting solid samples and layer-by-layer analysis.

EXPERIMENTAL

A Lyumas-30 time-of-flight mass spectrometer with the pulsed ionization of solid samples in a hollow cathode developed by Lyumeks was used in the experiments. Figure 1 shows a schematic diagram of the ion-optical system of this instrument.

A hollow-cathode source was used as an ionization source. Ions formed in the source together with neutral

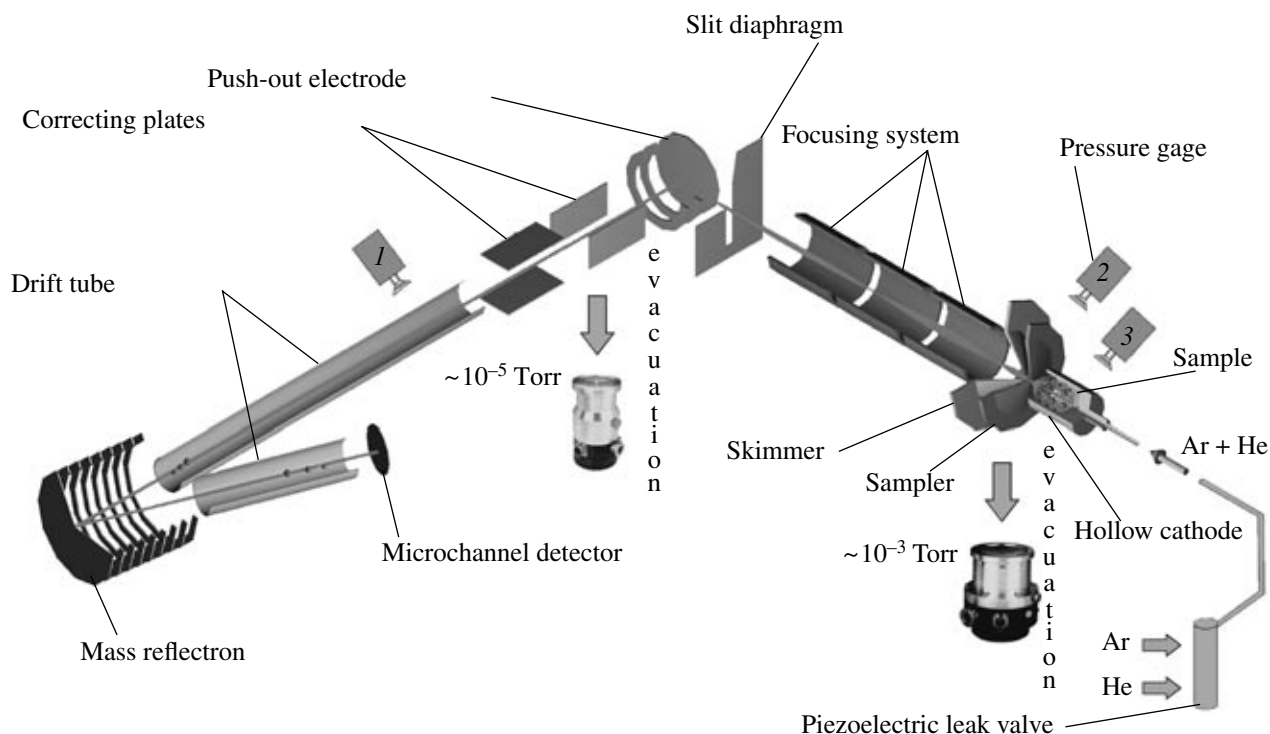


Fig. 1. Schematic diagram of the ion-optical system of a time-of-flight mass spectrometer.

atoms were transferred to a differential zone under the action of the small extraction voltage of a skimmer and a pressure difference (the pressure, which was measured by gage 2, in the differential zone between the sampler and the skimmer was equal to 10^{-3} Torr). In the differential zone, the major portion of neutral particles was removed by vacuum pumping and ions were collected at the slit diaphragm of the extraction zone with the use of a focusing system. A gas-dynamic component should be taken into consideration in the transfer of ions and neutral atoms to the slit diaphragm. The double pressure drop from several Torr to a pressure level of 10^{-5} – 10^{-6} Torr across specially shaped cone diaphragms (the sampler and the skimmer) resulted in the formation of a supersonic gas jet. A narrow ribbon-shaped ion beam, which was parallel to the extracting electrode, arrived at the extraction zone. Next, under the action of a push-out pulse, ions were injected into a high-voltage drift tube (in this high-vacuum part, the pressure was 10^{-5} – 10^{-6} Torr, as measured by pressure gage 1; this practically excluded collision processes in this zone), where they were separated in space and time with respect to time of flights depending on the ratio m/z . Thereafter, the ions reflected in a mass reflectron [25], which was used to enhance the resolving power of the spectrometer and arrived at the second high-voltage drift tube. They were detected on a collector with a chevron microchannel-plate assembly, the signal from which was amplified with a preamplifier and transferred to the digitization plate of a computer. The

amplitude discrimination of the additive noises of a preamplifier and an analog-to-digital converter was used in signal processing; this allowed us to remove them almost completely. It is well known that the pressure in the discharge cell strongly affects both the rate of sample sputtering and the rate of ionization of sputtered atoms. Therefore, to maintain stable conditions for analysis, the pressure of a ballast gas was stabilized with the use of pressure gage 3, which was mounted in the gas channel of the discharge cell. Data on the pressure measured to within 1% were transferred to a computer through an embedded controller; the computer stabilized the flow rate of the ballast gas over a specified range with a regulated piezoelectric leak valve. For this purpose, an ordinary control circuit was used, which allowed us to stabilize pressure in the discharge cell in 20–30 s. In this case, relative pressure variations were no higher than 2%. Table 1 summarizes the main technical parameters of the mass spectrometer.

An ionization source with a hollow cathode fully made of the sample material was developed for studying and further optimizing discharge parameters. Figures 2a and 2b show two versions of this source. A number of discharge parameters (discharge pulse duration, pulse repetition period, the pressure of a gas mixture in the discharge cell, and the ratio between the components of an Ar and He mixture) were optimized with the use of this source. However, note that layer-by-layer analysis and the analysis powder samples cannot be performed with the use of this source. Therefore, we

Table 1. Control voltages and parameters of a time-of-flight mass spectrometer with a hollow-cathode pulsed discharge

Cathode voltage	-1000 to -2000 V	Ionization pulse duration	1–300 μ s
Discharge current	to 3 A	Push-out pulse duration	0.1–2 μ s
Skimmer voltage	-50 to -100 V	Pulse frequency	100–10000 Hz
Push-out pulse voltage	+500 V	Sampler hole diameter	1–1.5 mm
Microchannel plate voltage	-2400 V	Skimmer hole diameter	1–1.5 mm
Flight tube voltage	to -2000 V	Discharge pressure	0.3–3 Torr

developed a source with a demountable cathode, which allowed us to perform this analysis (Fig. 2c).

The energy of ions arrived at the zone between the sampler and the skimmer from the cathode depends on the plasma potential and is approximately equal to 4–5 eV [5]. Because this energy does not allow one to efficiently focus an ion beam in the push-out zone, it should be increased considerably. For this purpose, a bias voltage across the cathode–anode pair with respect to a ground potential was introduced. The dependence of the component intensities of mass spectra on the bias voltage was practically the same for all masses, whereas the optimum bias voltage was equal to 18–20 V and almost independent of the type of the sample.

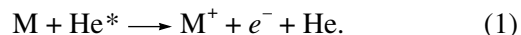
A ballast gas was introduced in three modes: through saw cuts in the bottom of the cathode walls (Fig. 2c), through a capillary arranged at the cathode axis (see Fig. 2a), and immediately into the discharge chamber (see Fig. 2b).

RESULTS AND DISCUSSION

Time discrimination of gas components. It was found [4, 5, 11] that the time discrimination of the emergence of sample ions with respect to the ions of gases present in the discharge was observed in either the Grimm discharge [4, 11] or a hollow cathode. Moreover, the time maximums of sample ions noticeably different in mass were somewhat different. This time discrimination requires the push-out pulse delay to

be optimized with respect to the discharge pulse. Figure 3 shows the dependence of the intensities of mass-spectroscopic lines for some ions on the push-out pulse delay interval. It can be seen that a compromise delay value of 70 μ s can be used for the majority of the elements. However, the concentrations of both light and heavy elements should often be monitored simultaneously in layer-by-layer analysis. Therefore, a detection mode with the jump delay was developed for layer-by-layer analysis; in this case, delays alternating from spectrum to spectrum were used.

Effect of hydrogen on the mass spectrum. In preliminary experiments on the use of various hollow-cathode versions for analytical purposes, it was found that the addition of helium (0.5–1.5 Torr) to argon excluded the appearance of a microcapillary discharge in channels through which a discharge gas is supplied to the cathode and increased the intensities of sample components by a factor of 2–3 [5]. It is likely that this increase is related to the appearance of an additional channel of the Penning ionization of the sample element M:



For this reason, in this study, we used a gas mixture of argon and helium in the discharge cell.

In a number of publications [26–28], the effect of an improvement in the crater shape in a sample upon the addition of a small amount of hydrogen (about 1%) to a gas mixture was described. Because of this, the layer-

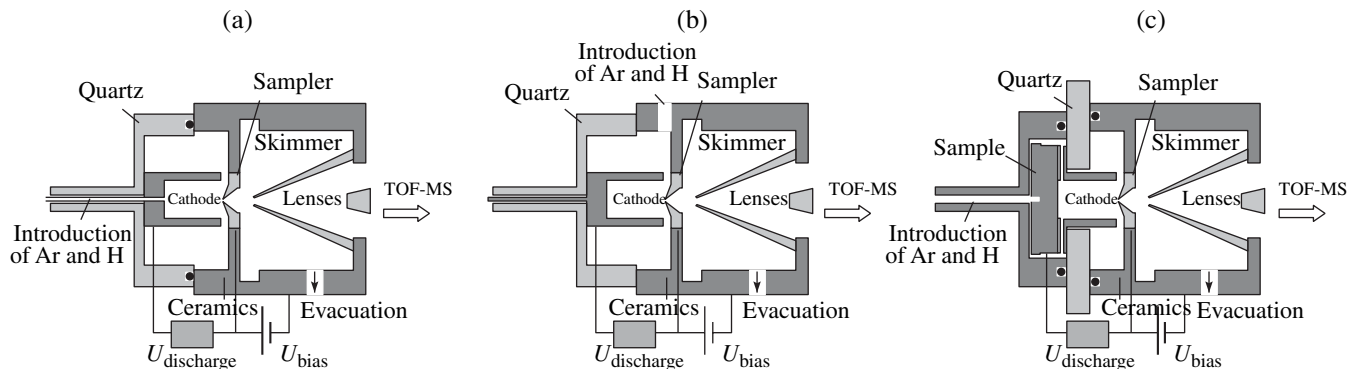


Fig. 2. Hollow-cathode ionization sources: (a) with the introduction of a ballast gas through a capillary at the central part of the cathode, (b) with the introduction of a gas outside the cathode, and (c) for layer-by-layer analysis and the analysis of nonconducting samples.

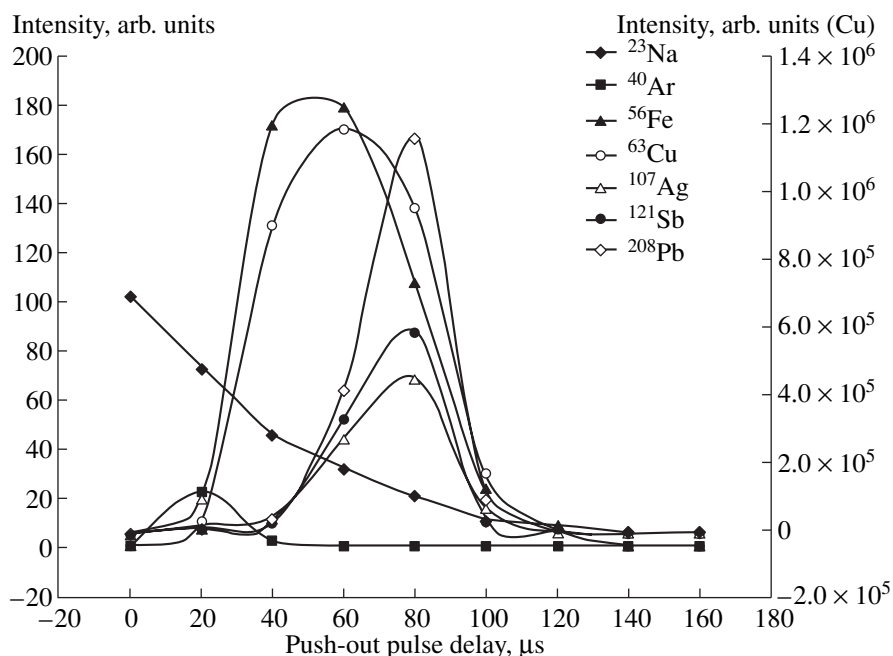


Fig. 3. Dependence of the intensities of the mass-spectrometric lines of ions on push-out pulse delay. $U_{\text{discharge}} = -1530$ V; $f = 1.4$ kHz; pulse duration of 5 μs ; $P_{\text{Ar}} = 1.6$ Torr; $P_{\text{He}} = 0.5$ Torr; accumulation time of 5 min (3×10^5 spectra).

by-layer sputtering of the sample material occurred more uniformly and conditions that prevent the formation of surface oxides were produced. Consequently, the efficiency of sample sputtering increased. Moreover, it was found [17, 29–31] that the addition of 1–10% hydrogen to a ballast gas several times increased the intensities of sample components (for a constant discharge). Mason et al. [29] noted a considerable increase (by a factor of up to 6) in the intensity of copper ions (the Grimm discharge with a copper cathode was used) upon the introduction of 1–20% hydrogen into the space between the discharge chamber and the sampler. In this case, hydrogen had no effect on sample sputtering. The intensities of gas components (Ar^+ , OH^+ , H_2O^+ , H_3O^+ , and ArH^+) considerably decreased in this case. In this context, we performed experiments in which hydrogen was added to the gas mixture used in the discharge chamber.

Figure 4 shows the dependence of the intensities of a number of sample components on the concentration of hydrogen. As can be seen in Fig. 4, unlike the results obtained by Mason et al. [29], the intensities for Sb^+ , Ag^+ , and Cu^+ changed only slightly. Changes that are more considerable were detected for aluminum (the intensity decreased by a factor of about 2) and lead (the intensity increased by a factor of 1.5). At the same time, the intensities of gas components (Ar^+ , OH^+ , H_2O^+ , H_3O^+ , and ArH^+) decreased many times upon the addition of hydrogen, as in the study by Mason et al. [29]. However, note that various clusters, such as CuArH , CuAlH , CuOH , CuOH_2 , CuOH_3 , and $\text{Al}_2\text{O}_3\text{H}$, appeared

in the spectrum upon the addition of relatively high concentrations of hydrogen (5–15%). Although the intensities of these clusters were lower than the intensities of the main components of the spectrum by 3–4 orders of magnitude, their presence noticeably impaired the analytical capabilities of the spectrometer.

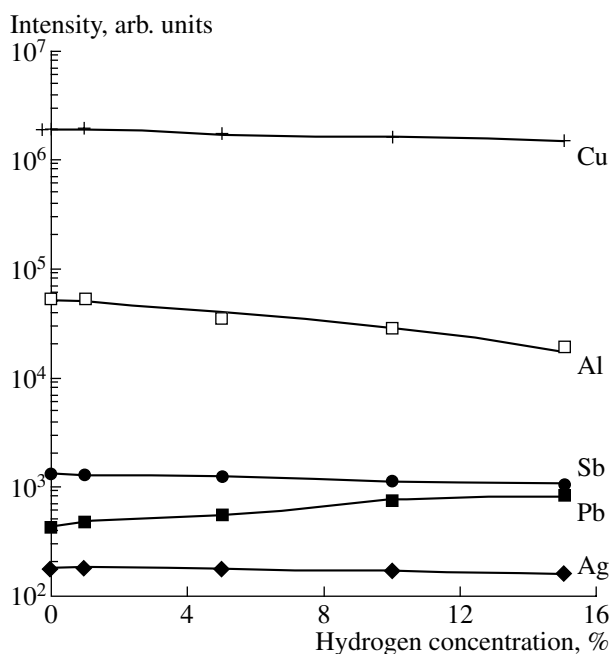


Fig. 4. Dependence of the intensities of the mass-spectrometric lines of ions on the concentration of hydrogen.

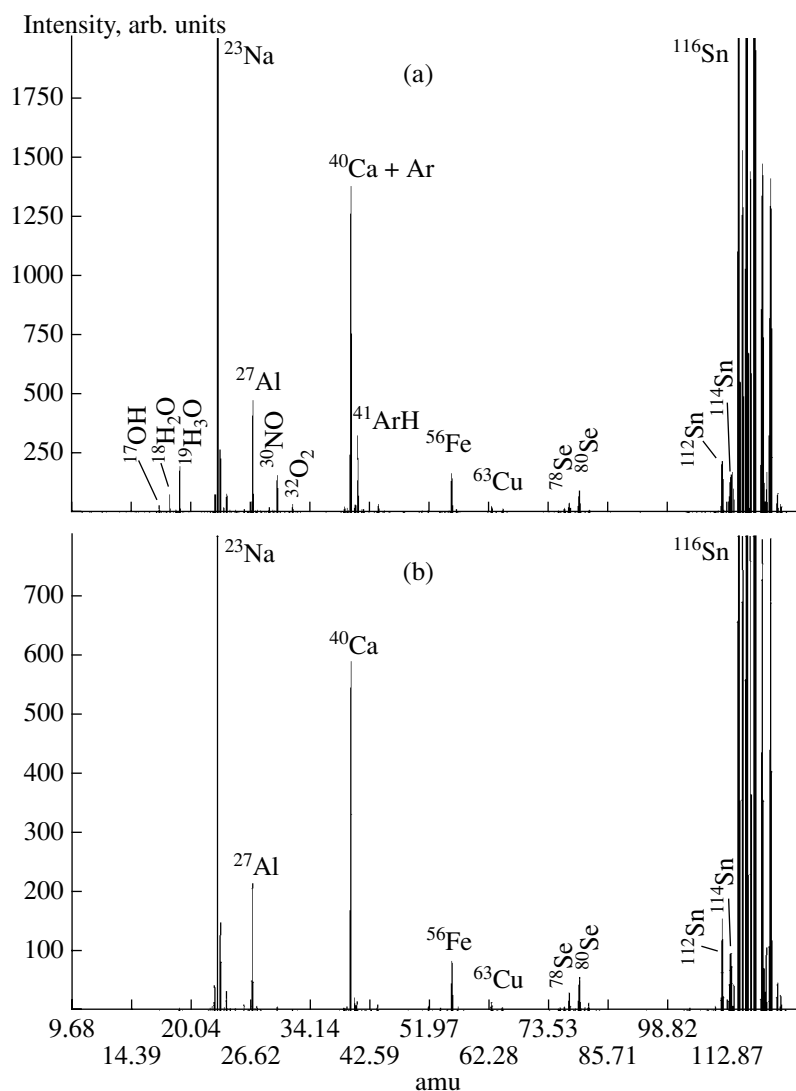


Fig. 5. Spectra of a lead–tin alloy in (a) pure Ar and (b) a mixture of Ar + He + H. In both cases, the pressure was 0.9 Torr and the accumulation time was 2 min (10^5 spectra).

Because of this, we used a gas mixture with a relatively low hydrogen content of 1% in subsequent experiments. In this case, we observed a considerable depression of gas components and, at the same time, hydride clusters were practically absent.

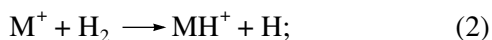
Figure 5 shows the spectra of a lead–tin alloy with various concentrations of a number of elements with the use of pure argon (Fig. 5a) or a gas mixture containing 70% argon, 29% helium, and 1% hydrogen as a ballast gas. The approximate concentrations of the elements (according to manufacturer's specifications) were as follows: Sb, 9%; Na, 0.3%; Ca, 0.1%; Cu, 0.007%; Se, 0.03%; and Fe, 0.02%. As can be seen in Fig. 5, the presence of hydrogen considerably decreased the intensities of gas components present in the mass spectrum; this significantly decreased interferences between gas components and sample elements (especially for light elements). Moreover, it can be seen

in Fig. 5a that high-purity argon, which was used as a discharge gas in this case, contained a relatively large amount of water, which was represented by a characteristic group in the mass spectrum (OH^+ , H_2O^+ , and H_3O^+), as well as by hydride clusters formed (ArH^+ , CuOH , CuOH_2 , and CuOH_3). In the presence of hydrogen, the gas components of the spectrum were suppressed (Fig. 5b). In particular, as can be seen in Fig. 5, the use of hydrogen allowed us to remove interference between ^{40}Ca and ^{40}Ar ; therefore, calcium could be determined in various samples with a high sensitivity (without the use of isotopes with low relative concentrations). In this case, a considerable decrease in the intensity of an argon component (by 2–3 orders of magnitude) in the spectra measured in other samples (without elements that interfere with ^{40}Ar) upon the addition of hydrogen suggests the absence of peak superposi-

tion. Hence, we can conclude that the peak at a mass of 40 shown in Fig. 5b corresponds to calcium and does not result from interference between ^{40}Ca and ^{40}Ar .

The mechanism of the influence of hydrogen on the components of a mass spectrum remains unclear. Previously [29, 32], attempts have been made to explain this phenomenon. However, it is our opinion that the explanation proposed is applicable to only a dc glow discharge (this discharge was considered in cited publications), whereas the phenomenon of an increase in the intensities of sample components and a decrease in the intensities of gas components has a more universal character, because it is also observed in both a radiofrequency discharge [31] and, in our case, a pulsed glow discharge.

In our opinion, this phenomenon can be related to the effect of hydrogen on the rates of recombination of various discharge components. The recombination of gas components in the presence of hydrogen can be explained by a two-step process. At the first step, the component ion is converted into the molecular ion with hydrogen:



at the second step, the recombination occurs as follows:



These processes significantly increase the rates of recombination of argon ions [33], because the molecular recombination cross sections are greater by several orders of magnitude than the direct atomic recombination cross section. We believe that these processes can also significantly increase the rates of recombination of gas components, such as OH and N_2 .

The increase in the intensity of sample ions upon the addition of hydrogen can be explained by an increase in the concentration of metastable Ar and H atoms in the course of process (2) and, thus, by an increase in the rate of the Penning ionization. The Penning ionization is a selective process: in this process, only atoms and molecules whose ionization energies are lower than the energy of a metastable level of Ar (14.1 eV) or H (10.2 eV) atoms undergo ionization. This condition is met for the majority of metal atoms; the ionization energies of most of them lie in the range 6–8 eV. Other components present in our discharge exhibited higher ionization potentials (10–13 eV, see Table 2).

Thus, the above mechanisms qualitatively describe a decrease in the intensity of gas components and an increase in the intensity of sample components in our and other types of gas discharges.

Mathematical treatment of mass spectra. To increase the resolving power of the mass spectrometer, we used the mathematical treatment of the experimental spectra based on the known instrument function. It

Table 2. Characteristic ionization energies of molecules and atoms

Molecule	Ionization energy, eV	Molecule	Ionization energy, eV
Ar	15.76	NH_2	11.14
H_2O	12.61	NH_3	10.7
H_2O_2	10.54	NO	9.75
N_2	15.58	NO_2	10.8
N_2O	12.8	O_2	12.07
NH	13.49	OH	13.0

is believed that the time dependence of the measured signal is determined by the following equation:

$$u(t) = \int K(t, t_0) f(t_0) dt_0, \quad (4)$$

where $u(t)$ is the measured signal, $K(t, t_0)$ is the instrument function, and $f(t)$ is the mass spectrum of the sample expressed on a time scale. Thus, the problem of increasing the resolving power is reduced to the problem of restoring the initial signal from a measured signal and the known instrument function. For this purpose, Eq. (4), which is an integral Fredholm equation of the first kind, should be solved. This problem is mathematically incorrect; however, there are numerical methods for solving problems of this kind [34]. Based on such methods, an algorithm was developed for restoring the initial mass spectrum: some isolated peak is chosen in the mass spectrum, and the instrument function is calculated based on this peak; next, this instrument function is stored in the main memory and written to a file. Thereafter, inverse convolution with specified parameters is performed to yield the restoration of the initial signal from the measured signal. Figure 6 shows measured and treated mass spectra. It can be seen that the mathematical treatment of the resulting signal resulted in a peak narrowing and, consequently, a considerable increase in the resolving power.

Analysis of high-purity copper. A number of elements in a sample of high-purity copper were determined with the use of the Lyumas-30 analyzer. For this purpose, the spectrometer was precalibrated using the M2p (No. 945) and M3 (No. 9410) certified reference samples of copper GOST (State Standard) 859-78. Table 3 summarizes the concentrations of the elements in these samples. Figure 7 shows the mass spectra obtained for the M3 copper. With the use of these samples, we obtained calibration functions for some elements. The sensitivities determined from calibration functions for various elements were found to be similar; they mainly fell in the range 3–6 ions per million for 10^6 pulses. Note that the relatively small difference in sensitivities for pulsed discharge mass spectrometry is related to the following two factors: (1) the relative concentrations of sputtered sample atoms in a gas phase are close to the corresponding concentrations in the

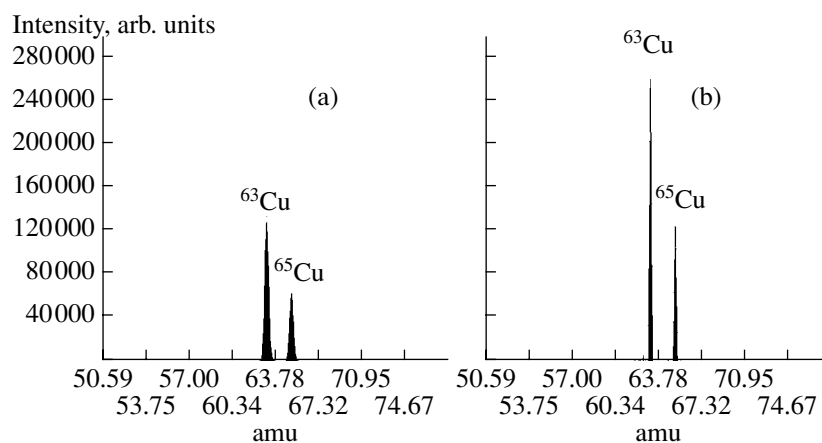


Fig. 6. Shapes of the components of a mass spectrum of ^{63}Cu and ^{65}Cu (a) before and (b) after mathematical treatment. The accumulation time was 15 min (10^6 spectra).

sample and (2) the rates of Penning ionization (in this case, the Penning ionization mechanism is predominant) are similar for different elements.

Figure 8 shows the mass spectra obtained for a high-purity copper sample, and Table 4 summarizes the concentrations of a number of elements. The concentrations of elements found using an ICP MS Element-2 analyzer (Thermo-Finnigan) are also given in Table 4. With the use of the Element-2 analyzer, a copper sample (0.05 g) was dissolved in purified nitric acid, and the resulting solution was diluted with deionized water to 1 L. Table 4 demonstrates that the results are satisfactorily coincident (the discrepancy between the results is no higher than 12%); this is indicative of the absence of systematic errors in the direct determination of element concentrations with the use of the Lyumas-30 analyzer.

Table 3. Concentrations (ppm) of the elements in standard copper samples

Element	Concentration in standard copper sample No. 945	Concentration in standard copper sample No. 9410
Ag	60	90
As	16	390
Bi	46	360
Cd	47	440
Cr	5	30
Fe	220	670
Mn	10	83
P	30	90
Pb	57	810
Sb	54	810
Si	6	33
Sn	100	760

Analysis of nonconducting samples. The version of a gas-discharge interface shown in Fig. 2c was used for the direct analysis of nonconducting samples. In this case, a sample as a flat disk was applied to a cylindrical cathode made of Nb, Ta, or Al. A gas mixture arrived at the discharge cell through saw cuts in the bottom of cathode walls. The cathode-wall material was chosen depending on the set of elements to be determined. Each of the elements of the cathode material produced its background spectrum. A cathode of aluminum exhibited the simplest spectrum. Aluminum (a component of mass 27) and Al_2O_3 (102) were present in the spectrum. When Nb and Ta were used, a number of oxides (NbO , NbO_2 , NbO_3 , TaO , TaO_2 , etc.) were observed in addition to the main components (93 and 181 for Nb and Ta, respectively). To illustrate the capabilities of a mass spectrometer with sample ionization by a short-pulsed discharge, we measured the spectra of glassy slag formed in the manufacture of lead. The composition of this slag should be known in order to develop a lead manufacturing process. Sample preparation was simple and consisted in cutting a disk from the test sample. Figure 9 shows the spectrum of this sample. As can be seen in Fig. 9, in addition to the main components (aluminum, lead, and oxygen), a number of other elements, in particular, S, Ca, Mg, Na, Fe, Mn, Co, Cr, K, and Ca, were also detected in the sample. Note that oxygen, which appeared in the spectrum as various oxides, is the oxygen that arrived at the discharge from the sample in the course of its sputtering. The above spectrum allowed us to perform only qualitative analysis: corresponding reference samples are required for quantitative determinations. However, long-developed reference samples can be used for calibration if the relative sensitivities for various elements are close to the relative sensitivities for conducting reference samples. Nevertheless, additional studies are required for testing this hypothesis.

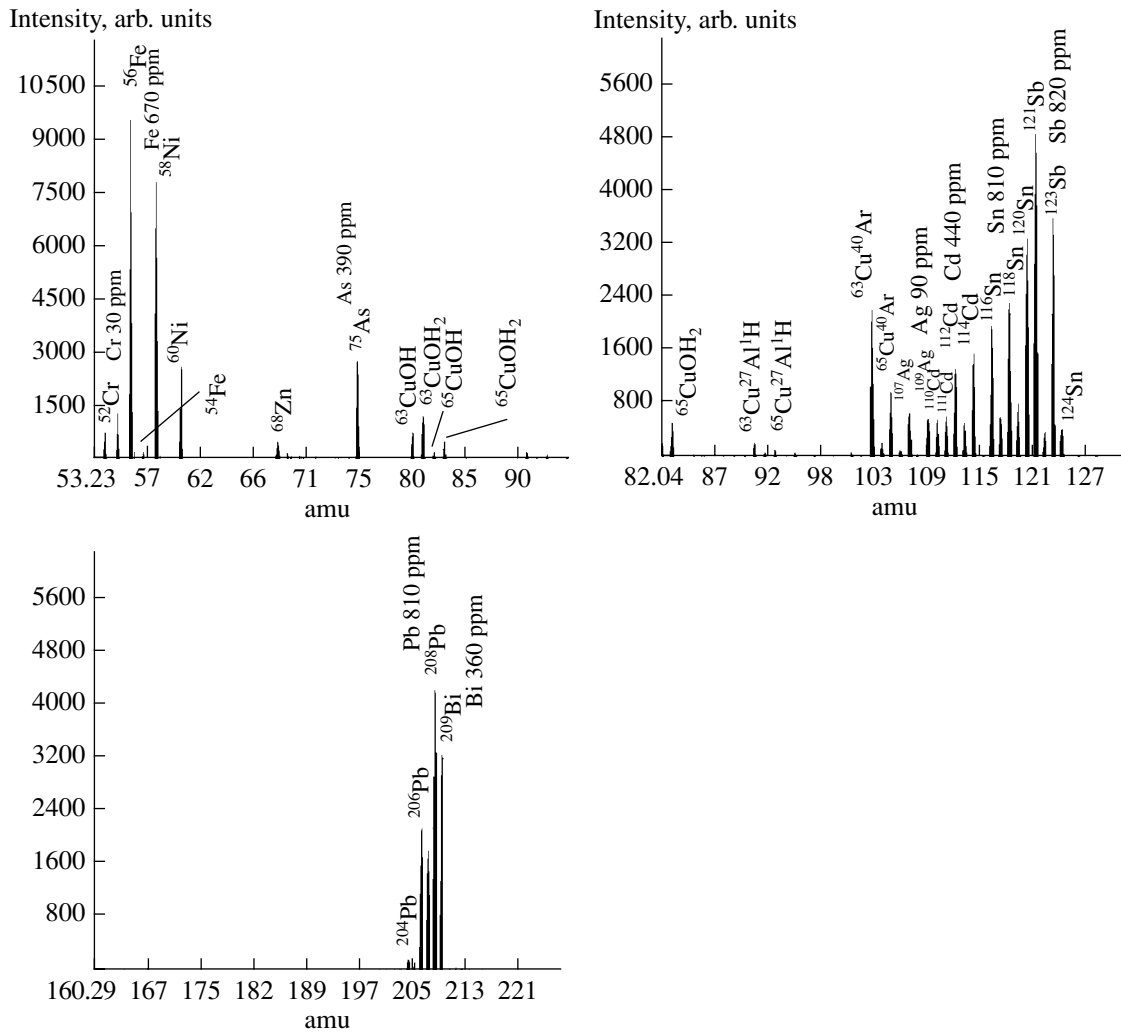


Fig. 7. Spectra of M3 standard copper sample No. 9410. $P_{\text{mixture}} = 2.5$ Torr (a mixture of 70% Ar, 29% He, and 1% H); $U_{\text{discharge}} = -1530$ V; $f = 1.6$ kHz; push-out pulse delay of 65 μs ; pulse duration of 3 μs ; analysis time of 10.5 min (10^6 spectra). The spectral region 62–64 amu is cut.

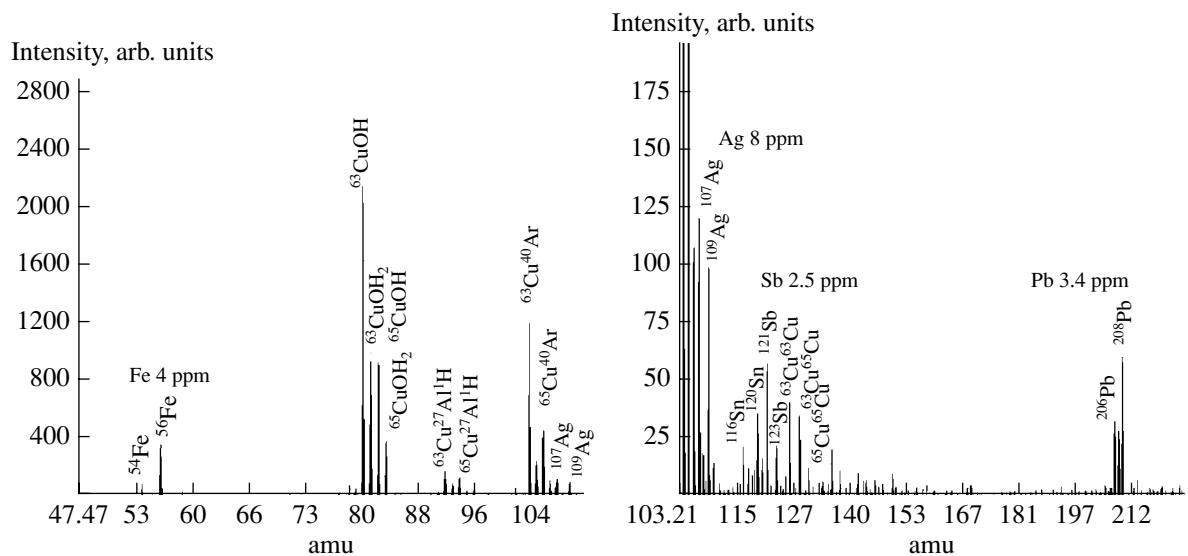


Fig. 8. Spectrum of a high-purity copper sample. $P_{\text{mixture}} = 2.5$ Torr (a mixture of 70% Ar, 29% He, and 1% H); $U_{\text{discharge}} = -1530$ V; $f = 1.6$ kHz; push-out pulse delay of 65 μs ; pulse duration of 3 μs ; analysis time of 21 min (2×10^6 spectra).

Table 4. Concentrations (ppm) of the elements in a high-purity copper sample

Element	Concentration in the high-purity copper sample (Lyumas-30)	Concentration in the high-purity copper sample (Element-2, Thermo-Finnigan)
Ag	8 ± 1	6.2 ± 0.3
Fe	0.4 ± 0.1	0.3 ± 0.04
Pb	0.4 ± 0.1	0.29 ± 0.02
Sb	<0.2	0.12 ± 0.02

Note: Measurement parameters: $P_{\text{mixture}} = 2.5$ Torr (a mixture of 70% Ar, 29% He, and 1% H); $U_{\text{discharge}} = -1530$ V; $f = 1.6$ kHz; push-out pulse delay of 65 μs ; pulse duration of 3 μs ; analysis time of 19 min (2×10^6 spectra); dark noise of <0.1 ion/mass (10^6 spectra).

Detection limits. Because noise is practically absent from the given system (the dark noise of a detector corresponds to a level lower than 0.1 ion/mass for 10^6 spectra, and the additive noise of an amplifier is eliminated by amplitude discrimination), the limits of detection were determined with the use of reference samples based on purely statistical criteria. In this case, the presence of only one ion corresponding to an element carries information on the presence of this element in the sample. To enhance reliability, we believed that the presence of three ions is convincing evidence for the presence of the test element. Table 5 summarizes the detection limits obtained in an optimized system.

The reproducibility of analytical results was determined as the relative standard deviation in six measure-

Table 5. Detection limits (ppm) of elements

Sample	Element	Detection limit
Copper	Pb	0.3
	Al	0.5
	Ni	0.3
	Sb	0.2
	Fe	0.2
	Ag	0.3
Lead	Fe	0.3
	Sb	0.3
	Na	0.6
	Ca	0.8

ments for each sample, and it was equal to 2–7% depending on the test element and its concentration in the sample.

CONCLUSIONS

The results of the study of a hollow-cathode pulsed glow discharge as an ion source for mass spectrometry demonstrate that it is applicable to the direct analysis of solid samples. Thus, a time-of-flight mass spectrometer with a hollow-cathode pulsed glow discharge is the most promising and efficient instrument for solving problems of current interest. This instrument is characterized by the most efficient use of a test sample (because sample atomization and ionization occur in a

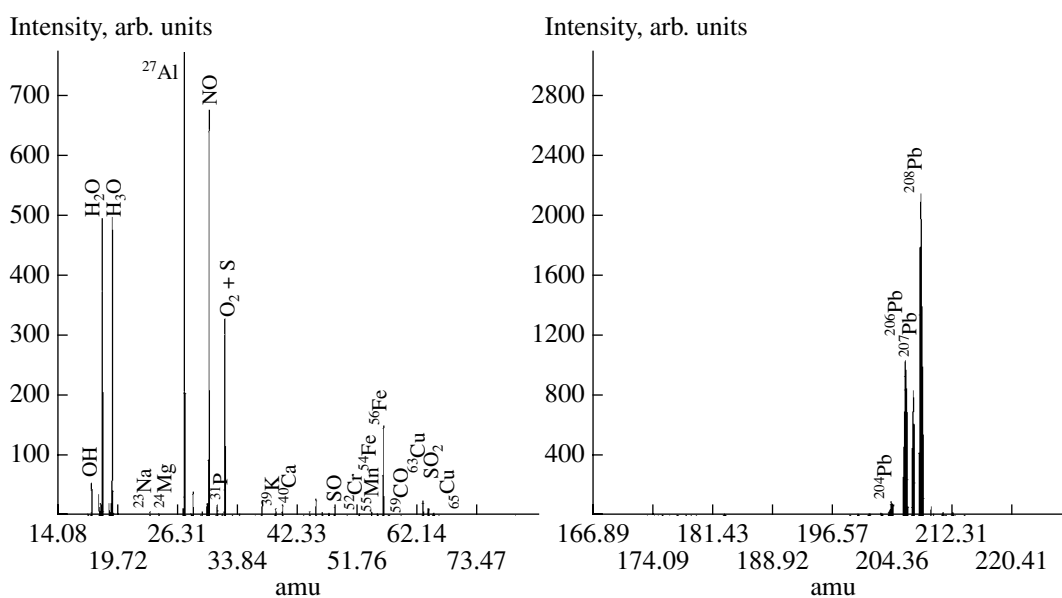


Fig. 9. Spectrum of a sample of glassy slag formed in the manufacture of lead (a mixture of 70% Ar, 29% He, and 1% H). $U_{\text{discharge}} = -1530$ V; $f = 1.6$ kHz; push-out pulse delay of 150 μs ; pulse duration of 3 μs ; analysis time of 10 min (10^6 spectra).

closed space), a higher efficiency of atomic ionization (because of an increased concentration of high-energy electrons), a much lower flow rate of the reaction gas (2–10 mL/min), a low electric power consumption (60–120 W), and the possibility of directly performing both the elemental analysis and the layer-by-layer analysis of conducting and dielectric substances and materials.

Note that this analyzer can be used in various areas of science and technology: in the atomic industry for the elemental and isotopic analysis of radionuclides, decay products, and nuclear wastes; in medicine, physics, electronics, and scientific research for isotope analysis in the manufacture and use of isotopically pure materials; in microelectronics for the determination of ultratrace impurity concentrations in superconducting materials (Si, As, Ga, etc.), including rapid (as compared with SIMS and AES techniques) layer-by-layer analysis of multilayer thin-film structures; in metallurgy for elemental analysis in the manufacture of non-ferrous metal alloys and special steels with regulated concentrations of trace impurities (including gaseous impurities); in the manufacture of high-purity materials for the elemental analysis of impurities in the manufacture of metals, optical glasses, optic fibers, alloys, and spray-coated surfaces; and in the analysis of mineral raw materials in concentration plants and the mining industry.

REFERENCES

1. Marcus, R., Anfone, A., Luesaiwong, W., Hill, T., Perahia, D., and Shimizu, K., *Anal. Bioanal. Chem.*, 2002, vol. 373, p. 656.
2. Drobyshev, A.I., *Zh. Prikl. Spektrosk.*, 1992, vol. 56, no. 1, p. 7.
3. Harrison, W.W., *Chem. Anal.*, 1988, vol. 95, p. 85.
4. Yang, C., Mohile, M., and Harrison, W.W., *J. Anal. At. Spectrom.*, 2000, vol. 15, p. 1255.
5. Potapov, S., Izrailov, E., Vergizova, V., Voronov, M., Suprunovich, S., Slyadnev, M., and Ganeev, A., *J. Anal. At. Spectrom.*, 2003, vol. 18, p. 564.
6. Van Straaten, M., Swenters, K., Gijbels, R., and Verlinden, J., *J. Anal. At. Spectrom.*, 1994, vol. 9, p. 1389.
7. Saito, M., *Spectrochim. Acta, B*, 1995, vol. 50, p. 171.
8. Duckworth, D.C., Barshick, C.M., and Smith, D.H., *J. Anal. At. Spectrom.*, 1993, vol. 8, p. 875.
9. Pelaez, M., Costa-Fernandez, J., Pereiro, R., Bordel, N., and Sanz-Medel, A., *J. Anal. At. Spectrom.*, 2003, vol. 18, p. 864.
10. De Gent, S., Van Grieken, R., Hang, W., and Harrison, W.W., *J. Anal. At. Spectrom.*, 1995, vol. 10, p. 689.
11. Harrison, W.W., Hang, W., Yan, X., and Ingenuity, K., *J. Anal. At. Spectrom.*, 1997, vol. 12, p. 891.
12. Puig, L. and Sacks, R., *Appl. Spectrosc.*, 1989, vol. 43, p. 801.
13. Venzago, C. and Weigert, M., *J. Anal. Chem.*, 1994, vol. 350, p. 303.
14. Grimm, W., *Spectrochim. Acta*, 1968, vol. 23, p. 443.
15. Harrison, W.W. and Bentz, B.L., *Prog. Anal. Spectrosc.*, 1988, vol. 11, p. 53.
16. Hang, W., Baker, C., Smith, B.W., Winefordner, J.D., and Harrison, W.W., *J. Anal. At. Spectrom.*, 1997, vol. 12, p. 143.
17. Pisonero, J., Turney, K., Bordel, N., Sanz-Medel, A., and Harrison, W.W., *J. Anal. At. Spectrom.*, 2003, vol. 18, p. 624.
18. Bengtson, A., *Spectrochim. Acta*, 1994, vol. 49, p. 411.
19. Payling, R. and Jones, D.G., *Surf. Interface Anal.*, 1993, vol. 20, p. 787.
20. Leach, A.M. and Hieftje, G.M., *J. Anal. At. Spectrom.*, 2000, vol. 15, p. 1121.
21. Ohata, M., Yasuda, H., Namai, Y., and Furuta, N., *Anal. Sci.*, 2002, vol. 18, p. 1105.
22. Charalambous, P.M., *Microchim. Acta*, 1987, vol. 91, p. 295.
23. Pisonero, J., Costa, J., Pereiro, R., Bordel, N., and Sanz-Medel, A., *Anal. Bioanal. Chem.*, 2004, vol. 379, p. 17.
24. Rümmele, M.H., Outred, M., Spillane, D.E.M., and Steers, E.B.M., *Fresenius' J. Anal. Chem.*, 1996, vol. 355, p. 820.
25. Mamyrin, B.A., Karataev, V.I., Shmikk, D.V., and Zagulin, V.A., *Zh. Eksp. Teor. Fiz.*, 1973, vol. 64, no. 1, p. 82.
26. Hodoroaba, V-D., Steers, E., Hoffmann, V., Unger, W., Paatsch, W., and Wetzig, K., *J. Anal. At. Spectrom.*, 2003, vol. 18, p. 521.
27. Fernandez, B., Bordel, N., Pereiro, R., and Sanz-Medel, A., *J. Anal. At. Spectrom.*, 2003, vol. 18, p. 151.
28. Menendez, A., Pisonero, J., Pereiro, R., Bordel, N., and Sanz-Medel, A., *J. Anal. At. Spectrom.*, 2003, vol. 18, p. 557.
29. Mason, R.S., Miller, P.D., and Mortimer, I.P., *Phys. Rev.*, 1997, vol. 55, p. 7462.
30. Saito, M., *Anal. Chim. Acta*, 1997, vol. 355, p. 129.
31. Tanaka, T., Matsuno, M., Woo, J.-C., and Kawagachi, H., *Anal. Sci.*, 1996, vol. 12, p. 591.
32. Newmann, K., Mason, R.S., Williams, D.R., and Mortimer, I.P., *J. Anal. At. Spectrom.*, 2004, vol. 19, p. 1192.
33. Raizer, Yu.P., *Fizika gazovogo razryada* (Physics of Gas Discharge), Moscow: Nauka, 1992.
34. Kalitkin, N.N., *Chislennye metody* (Numerical Methods), Moscow: Nauka, 1978.